Inorganic Chemistry

ARTICLE

pubs.acs.org/IC

Silicium Dioxide Nanoparticles As Carriers for Photoactivatable CO-Releasing Molecules (PhotoCORMs)

Gregor Dördelmann,[†] Hendrik Pfeiffer,[†,‡] Alexander Birkner,[§] and Ulrich Schatzschneider*[,†,‡]

[†]Lehrstuhl für Anorganische Chemie I - Bioanorganische Chemie, Ruhr-Universität Bochum, Universitätsstrasse 150, D-44801 Bochum, Germany

[‡]Institut für Anorganische Chemie, Julius-Maximilians-Universität Würzburg, Am Hubland, D-97074 Würzburg, Germany

[§]Lehrstuhl für Physikalische Chemie I, Ruhr-Universität Bochum, Universitätsstrasse 150, D-44801 Bochum, Germany

Supporting Information

ABSTRACT: Silicium dioxide nanoparticles of about 20 nm diameter containing azido groups at the surface were prepared by emulsion copolymerization of trimethoxymethylsilane and (3-azidopropyl)triethoxysilane and studied by transmission electron microscopy (TEM). A photoactivatable CO-releasing molecule (PhotoCORM) based on $[Mn(CO)_3(tpm)]^+$ (tpm = tris(pyrazolyl)methane) containing an alkyne-functionalized tpm ligand was covalently linked to the silicium dioxide nanoparticles via the copper-catalyzed azide−alkyne 1,3-dipolar cycloaddition (CuAAC "click" reaction). The surface functionalization of the particles with azido groups and manganese CORMs was analyzed by UV−vis, IR, ^1H and ^{13}C CP-MAS NMR spectroscopies as well as energy-dispersive X-ray spectroscopy (EDX). The myoglobin assay was used to demonstrate that the CORM-functionalized nanoparticles have photo-inducible CO-release properties very similar to the free complex. In the future, such functionalized silicium dioxide nanoparticles might be utilized as delivery agents for CORMs in solid tumors.

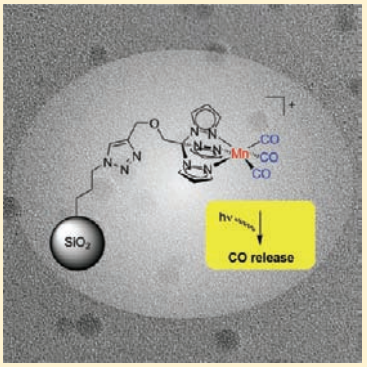

INTRODUCTION

Silicium dioxide nanoparticles find steadily increasing use as drug delivery systems due to their simple synthesis, biocompatibility, surface chemistry, and ease of size control.[1−4] Different techniques like encapsulation, covalent attachment, or adsorption can be used to immobilize therapeutic agents on these particles.[5,6] In particular, in cancer chemotherapy, nanoparticles are the focus of interest since they are able to passively target malignant tissue due to the unique pathophysiological characteristics of solid tumors like leaky vasculature and impaired drainage, which leads to an enhanced permeability and retention (EPR) of macromolecules in the tumor.[7−14] To also target the tumor tissue actively, peptides or antigens have been attached to the particle surface.[15] Thus, nanoparticles can improve site-specific drug delivery and reduce systemic exposure, giving rise to reduced side effects of chemotherapies. The ease of surface modification by copolymerization of tetraethylorthosilicate (TEOS) or related building blocks with different organo-trialkoxysilanes like (3-aminopropyl)triethoxysilane allows for various orthogonal synthetic strategies on the surface that are compatible with therapeutic agents as well as biological targeting molecules. Hence, silicium dioxide nanoparticles are a very promising platform to explore strategies for tumor drug delivery. To achieve additional spatial and temporal control of the bioactivity of such drug candidates, photochemical activation is a very attractive method and combining it with the targeting properties of silicium dioxide nanoparticles could bring special selectivity to such systems.[16] Among the many potential cytotoxic agents to attach to such a nanocarrier system, we thus selected a photoactivatable CO-releasing molecule (PhotoCORM) based on $[Mn(CO)_3(tpm)]$ (tpm = tris(pyrazolyl)methane.[17−21] Carbon monoxide is now well established as a small-molecule messenger in the human body and shows a delicate balance between cytoprotective and cytotoxic properties which can be exploited for therapeutic purposes.[22−28] At low concentrations, as generated by the heme oxygenases, the cytoprotective activity is dominant, while at very high systemic concentrations, as from inhalation of CO, toxicity to the whole organism occurs due to inference with oxygen transport and storage. However, at high local concentrations, for example, resulting from enrichment of CO-releasing molecules in tumor tissue, one should be able to achieve a cytotoxic effect which is beneficial in the sense that it kills the cancer cells but not the surronding tissue due to the limited mean diffusion length of the carbon monoxide. Since our PhotoCORM is not stable under the polymerization conditions used for nanoparticle synthesis, we utilized a mild conjugation reaction to attach it to the surface of the assembled nanoparticles, for which the copper-catalyzed azide−alkyne 1,3-dipolar cycloaddition (CuAAC, "click reaction") was selected. The CuAAC can be applied to multifunctional surfaces for orthogonal synthetic strategies and is compatible with many tumor cell-targeting molecules.[29−31] In

Received: December 3, 2010
Published: April 20, 2011

Scheme 1. Synthesis of 3-Azidopropyl-Functionalized Silicium Dioxide Nanoparticles by Emulsion Copolymerization of Trimethoxymethylsilane and (3-Azidopropyl)triethoxysilane Followed by Capping with Methoxytrimethylsilane and Hexamethyldisilazane[a]

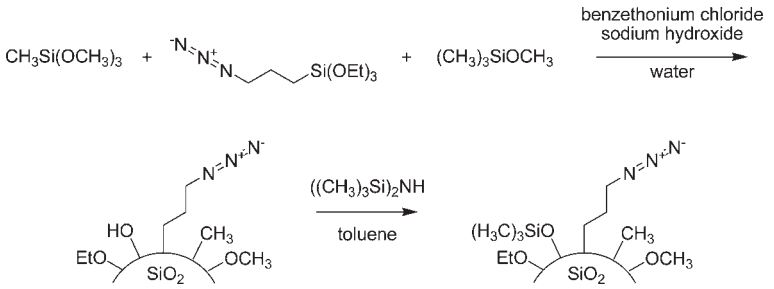

[a] The SiO_2-labeled half-sphere is to illustrate the silicium dioxide nanoparticles and the various surface functional groups.

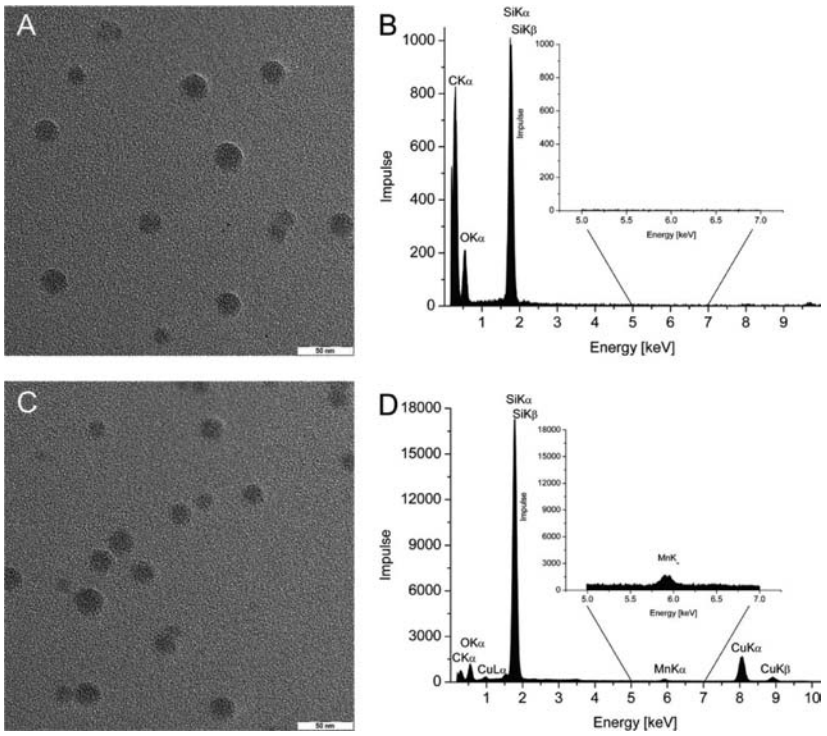

Figure 1. (A) TEM micrograph and (B) EDX spectrum of 3-azidopropyl-functionalized silicium dioxide nanoparticles. (C) TEM micrograph and (D) EDX spectrum of $[Mn(CO)_3(tpm\text{-}L1)]^+$-functionalized silicium dioxide nanoparticles.

addition, we already successfully employed it to couple the PhotoCORM to short carrier peptides.[19] To the best of our knowledge, this is the first report on CO-releasing molecules (CORMs) attached to nanoscale carriers.

RESULTS AND DISCUSSION

Precursor Synthesis. The (3-azidopropyl)triethoxysilane precursor was synthesized via a *Finkelstein* reaction. Catalytic amounts of potassium iodide were added to a solution of (3-chloropropyl)triethoxysilane and sodium azide in anhydrous dimethyl sulfoxide to give the desired product after 24 h of heating to reflux, while the reaction was incomplete without addition of potassium iodide under the same reaction conditions and even much longer reaction times. The reaction was followed by ^{1}H NMR spectroscopy and complete as indicated by the change in chemical shift of the triplet corresponding to the methylene group at the terminal CH_2N_3 position from 3.5 to 3.3 ppm upon substitution of chloride by azide. Furthermore, the IR spectrum showed the characteristic band for the organic azide at 2095 cm^{-1}.

3-Azidopropyl-Functionalized Nanoparticles. Silicium dioxide nanoparticles functionalized at the surface with the 3-azidopropyl group were prepared by the method of Tilley et al. via emulsion copolymerization of trimethoxymethylsilane and (3-azidopropyl)triethoxysilane (Scheme 1).[32]

This procedure provides a reproducible gram-scale synthesis of nanoparticles and proved to be advantageous to other methods in terms of starting material to solvent ratio, reaction time, and particle size.[33−35] A narrow size distribution with an average diameter of about 20 nm was determined by TEM (transmission electron microscopy), and also aggregation of particles was negligible for all particles prepare (Figure 1A and

dx.doi.org/10.1021/ic1024197 |*Inorg. Chem.* 2011, 50, 4362–4367

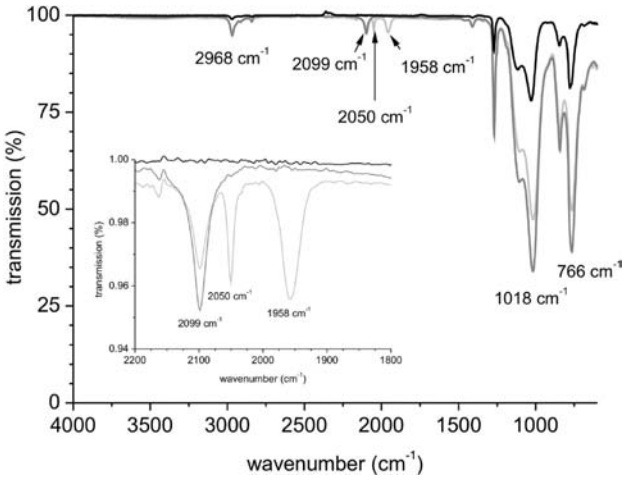

Figure 2. Overlay of the IR spectra of unfunctionalized (black) and 3-azidopropyl- (gray) and $[Mn(CO)_3(tpm\text{-}L1)]^+$-functionalized (light gray) silicium dioxide nanoparticles. (Inset) Region between 1800 and 2200 cm^{-1} with the characteristic bands of the azido (2099 cm^{-1}) and $Mn(CO)_3$ (1958 and 2050 cm^{-1}) groups.

1C). The EDX spectrum of the 3-azidopropyl-functionalized nanoparticles reflects the expected composition of the nanoparticles and shows the characteristic peaks for silicium and oxygen at 1.78 and 0.55 keV, respectively (Figure 1B).

The IR spectrum of the 3-azidopropyl-functionalized nanoparticles shows an additional band at 2099 cm^{-1} compared to the unfunctionalized particles (Figure 2), which indicates the presence of azido groups at the surface.

In the CP-MAS ^1H NMR, a reference sample of silicium dioxide nanoparticles capped with hexamethyldisilazane but without the 3-azidopropyl functionalization shows two signals at −0.11 and 3.65 ppm due to the $SiCH_3$ and $SiOCH_3$ groups, respectively (Figure S1, Supporting Information). The corresponding CP-MAS ^{13}C NMR shows two bands at −6.79 and 46.18 ppm. These are also due to the $SiCH_3$ and $SiOCH_3$ groups (Figure S2, Supporting Information). The 3-azidopropyl-functionalized nanoparticles, in the CP-MAS ^1H NMR, additionally show small shoulders at about 2.26 and 3.42 ppm corresponding to two of the three methylene groups of the 3-azidopropyl group in addition to the main $SiCH_3$ and $SiOCH_3$ peaks (Figure S3, Supporting Information). The third CH_2 signal could not be detected and is probably covered by the intense broad signal at −0.31 ppm of the $SiCH_3$ peak. Their CP-MAS ^{13}C NMR spectra, in addition to the signals at −6.60 and 46.26 ppm of $SiCH_3$ and $SiOCH_3$ moieties also visible in the spectra of the unmodified nanoparticles, display extra signals of the three methylene groups from the propyl linker at 1.85, 7.89, and 19.79 ppm (Figure S4, Supporting Information).[32]

$[Mn(CO)_3(tpm\text{-}L1)]PF_6$-Functionalized Nanoparticles. To couple the PhotoCORM $[Mn(CO)_3(tpm)]PF_6$ to the surface of the azido-functionalized nanoparticles, a derivative of the parent complex with an alkyne-substituted tpm ligand was utilized.[19] The copper-catalyzed azide−alkyne 1,3-dipolar cycloaddition (CuAAC) was performed in a 1:1:1 ethanol/*N*,*N*-dimethylformamide/water mixture using an excess of the metal carbonyl complex (Scheme 2). Even at rather long reaction times (96 h), the CuAAC reaction at the particle surface could not be brought to completeness, probably due to the inaccessibility of some surface site on the nanoparticles to the catalyst and/or CORM.

Scheme 2. Covalent Attachment of the $[Mn(CO)_3(tpm\text{-}L1)]^+$ Complex to the Surface of the (3-Azidoproply)-Functionalized Silicium Dioxide Nanoparticles via the Copper-Catalyzed Azide−Alkyne 1,3-Dipolar Cycloaddition (CuAAC)

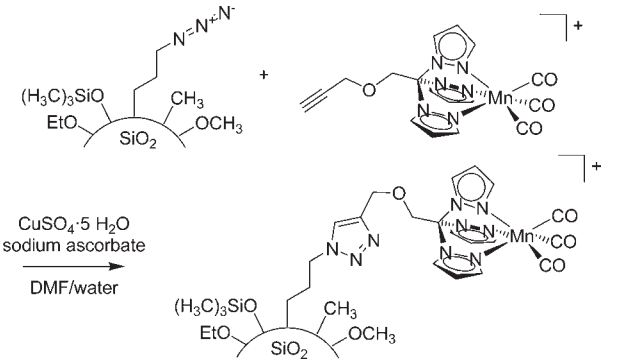

This is evident from the IR spectrum of the modified nanoparticles which in addition to the two C≡O vibrational bands characteristic of the $Mn(CO)_3$ moiety of the CORM at 1958 and 2050 cm^{-1} still shows the azido band at 2099 cm^{-1} (Figure 2), although of reduced intensity. In the ^{13}C CP-MAS NMR spectra, no additional signals could be detected compared to the 3-azidopropyl-functionalized particles, probably due to low loading and insufficient sensitivity of this method. However, the CP-MAS ^1H NMR spectrum shows a sharp signal at $\delta = 1.84$ ppm and a broad peak at around 6−9 ppm due to the methylene group and the three pyrazol protons, respectively. The latter, however, could not be resolved to individual peaks (Figure S5, Supporting Information). A TEM micrograph of the "clicked" nanoparticles is shown in Figure 1C. Compared to the 3-azidopropyl-functionalized nanoparticles, the CORM-functionalized particles have the same shape and size distribution, demonstrating that the particles are stable under the reaction conditions of the CuAAC (Figure 3A). The EDX spectrum (Figure 1D) displays an additional peak at 5.9 keV corresponding to the manganese of the $[Mn(CO)_3(tpm\text{-}L1)]^+$ moiety coupled to the surface via a triazole linkage. In addition, the metal-functionalized nanoparticles retain the yellow color of the parent complex even after extended washing, while the nonmodified particles are white (Figure 3B). The CHN and manganese content of the functionalized nanoparticles was determined with an elemental analyzer or atomic absorption spectroscopy (AAS), respectively. Samples were found to contain 0.50% (w/w) of manganese and 2.47% (w/w) of nitrogen. This converts to a content of 0.09 mmol of manganese per 1 g of nanoparticle and 1.76 mmol/g of nitrogen. If one assumes that all manganese is exclusively present in the form of $[Mn(CO)_3(tpm)]^+$, then 0.54 mmol/g of the total nitrogen should be due to the tpm ligands, leaving 1.22 mmol/g of nitrogen. If one assumes that this is all in the form of azide or triazole, there should be 0.41 mmol/g of these functional groups on the nanoparticle. Thus, the degree of surface functionalization with the $[Mn(CO)_3(tpm)]^+$ moiety can be estimated as approximately 22% (0.09/0.41·100). Although there are other sources of nitrogen around during the synthesis which might remain in the sample in unknown quantities, this result is in surprisingly good agreement with the decrease of the intensity of the azide band at 2099 cm^{-1} in the IR spectra of the azide vs the "clicked" nanoparticles (inset in Figure 2).

dx.doi.org/10.1021/ic1024197 |*Inorg. Chem.* 2011, 50, 4362–4367

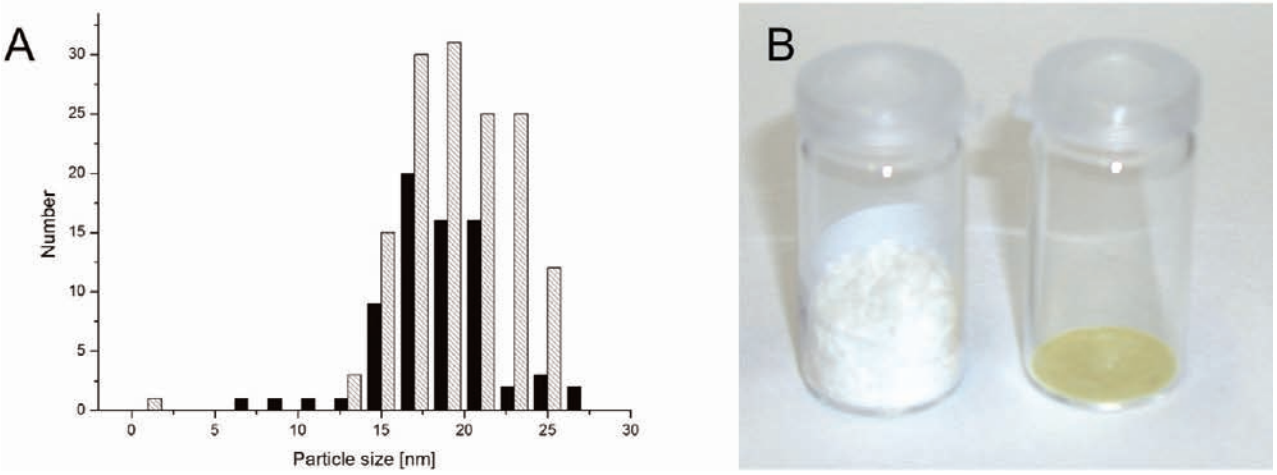

Figure 3. (A) Size distribution of 3-azidopropyl- (shaded) and $[Mn(CO)_3(tpm\text{-}L1)]^+$-functionalized silicium dioxide nanoparticles (black). (B) Photograph of samples of 3-azidopropyl- (left) and $[Mn(CO)_3(tpm\text{-}L1)]^+$-functionalized silicium dioxide nanoparticles (right).

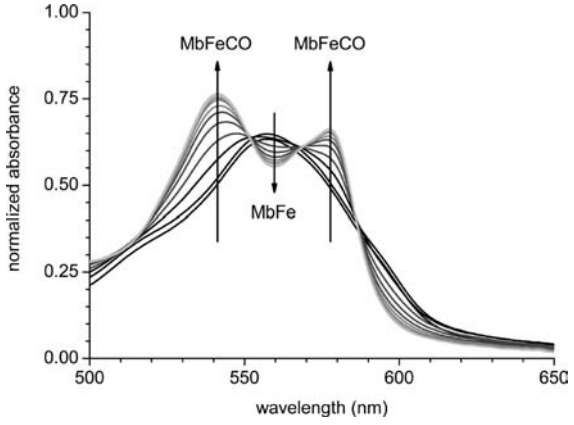

Figure 4. Normalized UV−vis absorption spectra of a solution of $[Mn(CO)_3(tpm)]^+$-functionalized silicium dioxide nanoparticles (0.4 mg) and reduced horse skeletal myoglobin (50 μM) in 0.1 M phosphate buffer upon irradiation at 365 nm (t = 0−85 min). MbFe is the reduced ferrous form of myoglobin and MbFeCO the carbon monoxide adduct thereof. The arrows indicate the change in absorption intensity during the course of the irradiation.

CO-Release Properties. The CO-release properties of the CORM-functionalized nanoparticles were investigated with the myoglobin assay. Thus, a buffered aqueous solution of horse skeletal myoglobin (MbFe) was freshly reduced with excess sodium dithionite under nitrogen, and then, the CORM-nanoparticles were added. When kept in the dark, no spectral changes could be observed over 15 h except of some general decrease in absorption intensity, probably due to partial sedimentation of the nanoparticles (Figures S6 and S7, Supporting Information). In contrast, upon irradiation at 365 nm, spectral changes characteristic of CO binding to the iron center in MbFe were observed in the Q-band region. The MbFe band at 560 nm decreased in intensity, while the two bands at 540 and 579 nm increased with irradiation time, indicating conversion of MbFe to MbFeCO (Figures 4 and S8, Supporting Information). No quantitative evaluation of the amount of CO released is possible since these experiments have to be carried out under saturation conditions with an excess of nanoparticle-bound manganese carbonyl present over myoglobin. However, the free compound was shown to release between 2 and 3 equiv of carbon monoxide per mole of complex.[19]

CONCLUSION

In the present work, we demonstrated that azido-modified silicium dioxide nanoparticles can be utilized as a carrier system for the photoactivatable CO-releasing molecule (PhotoCORM) $[Mn(CO)_3(tpm)]^+$. Surface functionalization was achieved via a copper-catalyzed 1,3-dipolar azide−alkyne cycloaddition (CuAAC) with a complex carrying an alkyne-modified tpm ligand, which allows for orthogonal synthetic strategies at the surface, and was demonstrated by EDX spectroscopy, showing the peak of manganese at 5.9 keV, as well as IR spectroscopy, with two C≡O bands at 1958 and 2050 cm^{-1} indicating the presence of the intact $Mn(CO)_3$ moiety. However, despite extended reaction times, the reaction was not complete, as indicated by some residual intensity of the vibrational signal of the azido group at 2099 cm^{-1}, probably due to the inaccessibility of some of the surface azido groups to the catalyst and/or CORM. With the myglobin assay, we were able to show that the CORM-functionalized nanoparticles were stable in the dark in aqueous buffer for several hours and upon photoactivation show CO-release properties very similar to the free complex. In further biological experiments, the utility of these systems for CO delivery to tumor tissue will be evaluated.

EXPERIMENTAL SECTION

Materials and Methods. Reactions were carried out in oven-dried Schlenk glassware under an atmosphere of pure nitrogen when necessary. Solvents were dried over molecular sieves and degassed prior to use. All chemicals were obtained from commercial sources and used without further purification. NMR spectra of molecular precursors and the manganese CORM were recorded on Bruker DPX 200 and DRX 400 spectrometers (^{1}H at 200.13 and 400.13 MHz, respectively; ^{13}C at 50.33 and 100.62 MHz). NMR spectra of the nanoparticles were recorded on a Bruker DSX-400 MAS spectrometer (^{1}H at 399.94 and ^{13}C at 100.58 MHz) using a VTN 2.5 mm MAS probehead and a rotation frequency of 20 kHz. Solution chemical shifts δ in ppm represent a downfield shift relative to tetramethylsilane (TMS) and were referenced relative to the signal of the solvent.[36,37] The solid state NMR spectra were referenced

dx.doi.org/10.1021/ic1024197 |Inorg. Chem. 2011, 50, 4362–4367

against adamantane for both ^{1}H and ^{13}C. Coupling constants J are given in Hertz. Individual peaks are marked as singlet (s), doublet (d), triplet (t), quartet (q), or multiplet (m). The IR spectra were recorded on pure solid samples with a Bruker Tensor 27 IR spectrometer equipped with a Pike MIRacle Micro ATR accessory. Transmission electron microscopy (TEM) and energy-dispersive X-ray spectroscopy (EDX) were performed using a Hitachi H-8100 microscope equipped with an EDX spectrometer from Oxford Instruments operating at an accelerating voltage of 200 keV. Samples were prepared by dispersing a small amount of the nanoparticles in ethanol (5 mL), followed by sonication for 30 min and deposition on copper or gold grids with a carbon support film. The CHN and manganese determinations were carried out by the Labor für Mikroanalytik and Thermoanalyse of the Universität Duisburg-Essen using a Euro EA elemental analyzer from Euro Vector Instruments and a M-Series atomic absorption spectrometer (AAS) from Thermo Electron, respectively. The myoglobin assay was carried out in a quartz cuvette (d = 1 cm) using a Jasco V-670 UV−vis spectrometer as described below.

(3-Azidopropyl)triethoxysilane 1. An oven-dried Schlenk flask was charged with (3-chloropropyl)-triethoxysilane (2.7 g, 11.2 mmol, 1 equiv), sodium azide (1.4 g, 22.4 mmol, 2 equiv), and sodium iodide (0.3 g, 0.7 mmol). Anhydrous dimethyl sulfoxide (20 mL) was added, and the mixture was heated to 60 °C for 24 h under a nitrogen atmosphere. After cooling to room temperature, hexane (20 mL) was added and the mixture was stirred vigorously for 2 h before the organic layers were allowed to separate. The hexane layer was washed with water (3 × 10 mL) and brine (1 × 10 mL) and then dried over magnesium sulfate. Removal of the solvent under vacuum gave (3-azidopropyl)-triethoxysilane (**1**) as a colorless oil. Yield: 41% (1.14 g, 4.6 mmol). IR (ATR, cm^{-1}): 2970, 2095, 1074, 955, 775. ^{1}H NMR (200.13 MHz, $CDCl_3$) δ 3.83 (q, 6H, $SiOCH_2$, J = 7.0 Hz,), 3.27 (t, 2H, CH_2N_3, J = 6.9 Hz), 1.83−1.61 (m, 2H), 1.23 (t, 9H, CH_2CH_3, J = 7.0 Hz), 0.76−0.61 (m, 2H, $SiCH_2$).

3-Azidopropyl-Functionalized Nanoparticles. A round-bottom flask was charged with benzethonium chloride (0.384 g, 0.86 mmol), solid sodium hydroxide (0.005 g, 0.13 mmol), and water (100 mL). The solution was stirred vigorously for 5 min, and then methyltrimethoxysilane (4.5 g, 33.0 mmol) and (3-azidopropyl)triethoxysilane **1** (0.5 g, 2 mmol) were added dropwise over 5 min. The emulsion was stirred vigorously for 5 h before methoxytrimethylsilane (1.6 mL, 0.012 mmol) was added. After stirring for an additional 12 h, the emulsion was added to a crystallizing dish charged with methanol (200 mL). Filtration of the precipitate formed followed by copious rinsing with methanol gave a colorless powder. The particles were then dispersed in toluene (60 mL), hexamethyldisilazane (2.1 mL, 0.010 mmol) was added, and the solution was stirred for an additional 16 h. The solution was then poured into methanol (200 mL). Collection of the precipitate followed by drying under vacuum gave the nanoparticles as a white powder. Yield: 1.76 g. IR (ATR, cm^{-1}): 2968, 2099, 1269, 1018, 766. ^{1}H CP-MAS NMR (399.94 MHz): δ = 3.76 ($SiOCH_3$), 3.42 (CH_2N_3, very weak), 2.26 (CH_2), −0.31 ($SiCH_3$). The third methylene group of the propyl chain could not be resolved. ^{13}C CP-MAS NMR (100.58 MHz): δ 50.62 ($SiOCH_2CH_3$), 46.26 ($SiOCH_3$), 19.79 (CH_2), 7.89 (CH_2), 1.85 (CH_2), −6.60 ($SiCH_3$).

$[Mn(CO)_3(tpm)]^+$-Functionalized Nanoparticles. A Schlenk flask was charged with $[Mn(CO)_3(tpm\text{-}L1)]PF_6$ (20 mg, 0,036 mmol),[19] 3-azidopropyl-functionalized nanoparticles (56.4 mg) suspended in ethanol (1 mL), sodium ascorbate (0.75 mg, 3.8 μmol), and copper(II)sulfate-pentahydrate (0.1 mg, 3.8 μmol). Then, *N*,*N*-dimethylformamide (1 mL) and water (1 mL) were added, and the mixture was stirred at room temperature under a nitrogen atmosphere for 96 h with exclusion of light. The mixture was then centrifuged (13 500 rpm, 2 min), and the resulting yellow precipitate was washed with methanol (5 × 2 mL). Drying under vacuum gave the CORM-functionalized nanoparticles as a yellow powder. Yield: 46.7 mg. IR (ATR, cm^{-1}): 2968, 2099, 2050, 1958, 1269, 1018, 766. ^{1}H CP-MAS NMR (399.94 MHz): δ 6−9 (broad, pyrazole-$H_{3,4,5}$), 4.21 ($SiOCH_3$), 1.84 (CH_2), 0.79 ($SiCH_3$). Elemental analysis (%): C, 20.73; H, 5.25; N, 2.47. M_n 0.50.

Myoglobin Assay. A solution of horse skeletal myoglobin (56.9 μM, 879 μL) in phosphate buffer (0.1 M, pH 7.3) was degassed by bubbling with nitrogen and then reduced by addition of an excess (200 equiv) of sodium dithionite (100 mM, 100 μL) in phosphate buffer (0.1 M, pH 7.3). Then, a dispersion of the $[Mn(CO)_3(tpm)]^+$-functionalized nanoparticles (0.4 mg, 10 μL) in dimethyl sulfoxide was added, followed by phosphate buffer to give a total volume of 1 mL with final concentrations of 50 μM myoglobin, 10 mM sodium dithionite, and 0.4 mg/mL of nanoparticles. The sealed cuvette was either kept in the dark as a control experiement or irradiated under nitrogen with an UV hand lamp at 365 nm, positioned perpendicular to the cuvette in a distance of 5 cm. The irradiation was interrupted in 5 min intervals to take UV−vis spectra on a Jasco V-670 spectrometer until no more changes in the Q-band region were observed. Finally, the solution was saturated with CO gas by bubbling to test whether conversion to MbFeCO was complete.

■ ASSOCIATED CONTENT

Supporting Information. CP-MAS ^{1}H and ^{13}C NMR spectra of nonmodified as well as 3-azidopropyl- and $[Mn(CO)_3(tpm)]^+$-functionalized silicium dioxide nanoparticles (Figures S1−S5); UV−vis spectra and change in absorption intensity of $[Mn(CO)_3(tpm)]^+$-functionalized silicium dioxide nanoparticles upon incubation in phosphate buffer in the dark and after irradiation at 365 nm (Figures S6−S8). This material is available free of charge via the Internet at http://pubs.acs.org.

■ AUTHOR INFORMATION

Corresponding Author

*E-mail: ulrich.schatzschneider@uni-wuerzburg.de.

■ ACKNOWLEDGMENT

This work was supported by the Deutsche Forschungsgemeinschaft (DFG) within FOR 630 "Biological function of organometallic compounds" and the Research Department Interfacial Systems Chemistry (RD IFSC) of the Ruhr-Universität Bochum (RUB). U.S. thanks Prof. Dr. Nils Metzler-Nolte (Bochum) for generous access to the research infrastructure of his work group.

■ REFERENCES

(1) Lu, J.; Liong, M.; Sherman, S.; Xia, T.; Kovochich, M.; Nel, A. E.; Zink, J. I.; Tamanoi, F. *Nanobiotechnology* **2007**, *3*, 89–95.

(2) Finnie, K. S.; Bartlett, J. R.; Barbe, C. J. A.; Kong, L. G. *Langmuir* **2007**, *23*, 3017–3024.

(3) Kumar, R.; Roy, I.; Ohulchanskyy, T. Y.; Goswami, L. N.; Bonoiu, A. C.; Bergey, E. J.; Tramposch, K. M.; Maitra, A.; Prasad, P. N. *ACS Nano* **2008**, *2*, 449–456.

(4) Selvan, S. T.; Tan, T. T. Y.; Yi, D. K.; Jana, N. R. *Langmuir* **2010**, *26*, 11631–11641.

(5) Vallet-Regi, M.; Balas, F.; Arcos, D. *Angew. Chem., Int. Ed.* **2007**, *46*, 7548–7558.

(6) Manzano, M.; Colilla, M.; Vallet-Regi, M. *Expert Opin. Drug Delivery* **2009**, *6*, 1383–1400.

(7) Maeda, H.; Greish, K.; Fang, J. *Adv. Polym. Sci.* **2006**, *193*, 103–121.

(8) Maeda, H. *Bioconjugate Chem.* **2010**, *21*, 797–802.

(9) Matsumura, Y.; Maeda, H. *Cancer Res.* **1986**, *461*, 6387–6392.

(10) Baban, D. F.; Seymour, L. W. *Adv. Drug Delivery Rev.* **1998**, *34*, 109–119.

(11) Maeda, H.; Wu, J.; Sawa, T.; Matsumura, Y.; Hori, K. *J. Controlled Release* **2000**, *65*, 271–284.
(12) Brigger, I.; Dubernet, C.; Couvreur, P. *Adv. Drug Delivery Rev.* **2002**, *54*, 631–651.
(13) Torchilin, V. P. *AAPS J.* **2007**, *9*, E128–E147.
(14) Rivera, G. P.; Parak, W. J. *ACS Nano* **2008**, *2*, 2200–2205.
(15) Rosenholm, J. M.; Sahlgren, C.; Linden, M. *Nanoscale* **2010**, *2*, 1870–1883.
(16) Celli, J. P.; Spring, B. Q.; Rizvi, I.; Evans, C. L.; Samkoe, K. S.; Verma, S.; Pogue, B. W.; Hasan, T. *Chem. Rev.* **2010**, *110*, 2795–2838.
(17) Schatzschneider, U. *Inorg. Chim. Acta* **2011**, in print; doi:10.1016/j.ica.2011.02.068
(18) Niesel, J.; Pinto, A.; Peindy N′Dongo, H. W.; Merz, K.; Ott, I.; Gust, R.; Schatzschneider, U. *Chem. Commun.* **2008**, 1798–1800.
(19) Pfeiffer, H.; Rojas, A.; Niesel, J.; Schatzschneider, U. *Dalton Trans.* **2009**, 4292–4298.
(20) Rimmer, R. D.; Richter, H.; Ford, P. C. *Inorg. Chem.* **2010**, *49*, 1180–1185.
(21) Meister, K.; Niesel, J.; Schatzschneider, U.; Metzler-Nolte, N.; Schmidt, D. A.; Havenith, M. *Angew. Chem.* **2010**, *122*, 3382–3384.
(22) Mann, B. E. . In *Topics in Organometallic Chemistry*; Metzler-Nolte, N., Jaouen, G., Eds.; Springer: Berlin, 2010; Vol. 32, pp 247−285.
(23) Motterlini, R.; Otterbein, L. E. *Nat. Rev. Drug Discovery* **2010**, *9*, 728–743.
(24) Johnson, T. R.; Mann, B. E.; Clark, J. E.; Foresti, R.; Green, C. J.; Motterlini, R. *Angew. Chem., Int. Ed.* **2003**, *42*, 3722–3729.
(25) Motterlini, R.; Mann, B. E.; Foresti, R. *Expert Opin. Invest. Drugs* **2005**, *14*, 1305–1318.
(26) Boczkowski, J.; Poderoso, J. J.; Motterlini, R. *Trends Biochem. Sci.* **2006**, *31*, 614–621.
(27) Alberto, R.; Motterlini, R. *Dalton Trans.* **2007**, 1651–1660.
(28) Mann, B. E.; Motterlini, R. *Chem. Commun.* **2007**, 4197–4208.
(29) Bräse, S.; Gil, C.; Knepper, K.; Zimmermann, V. *Angew. Chem., Int. Ed.* **2005**, *44*, 5188–5240.
(30) Kolb, H. C.; Sharpless, K. B. *Drug Discovery Today* **2003**, *8*, 1128–1137.
(31) Hong, V.; Presolski, S. I.; Ma, C.; Finn, M. G. *Angew. Chem.* **2009**, *121*, 10063–10067.
(32) Bradley, C. A.; Yuhas, B. D.; McMurdo, M. J.; Tilley, T. D. *Chem. Mater.* **2009**, *21*, 174–185.
(33) Liong, M.; Lu, J.; Kovochich, M.; Xia, T.; Rühm, S. G.; Nel, A. E.; Tamanoi, F.; Zink, J. I. *ACS Nano* **2008**, *2*, 889–896.
(34) Bagwe, R. P.; Hilliard, L. R.; Tan, W. *Langmuir* **2006**, *22*, 4357–4362.
(35) Fan, H. Y.; Lu, Y. F.; Stump, A.; Reed, S. T.; Baer, T.; Schunk, R.; Perez-Luna, V.; Brinker, C. J. *Nature* **2000**, *405*, 56–60.
(36) Gottlieb, H. E.; Kotlyar, V.; Nudelman, A. *J. Org. Chem.* **1997**, *62*, 7512–7515.
(37) Fulmer, G. R.; Miller, A. J. M.; Sherden, N. H.; Gottlieb, H. E.; Nudelman, A.; Stoltz, B. M.; Bercaw, J. E.; Goldberg, K. I. *Organometallics* **2010**, *29*, 2176–2179.